Available online at www.sciencedirect.com

ScienceDirect

Ceramics International 40 (2014) 3933–3937

CERAMICS INTERNATIONAL

www.elsevier.com/locate/ceramint

Phase transitions in $(1-x)BaZr_{0.2}Ti_{0.8}O_3-xBa_{0.7}Ca_{0.3}TiO_3$ powders and ceramic pellets

W. Wang, W.L. Li, D. Xu, W.P. Cao, Y.F. Hou, W.D. Fei*

School of Materials Science and Engineering, Harbin Institute of Technology, Harbin 150001, PR China

Received 3 August 2013; received in revised form 4 August 2013; accepted 7 August 2013
Available online 15 August 2013

Abstract

The phase transitions in $(1-x)BaZr_{0.2}Ti_{0.8}O_3-xBa_{0.7}Ca_{0.3}TiO_3$ (BZT-*x*BCT) powders and ceramic pellets were studied. It is found that the phase compositions in the pellets are different from that in the powders, which may be caused by the stress in the pellets. The monoclinic phase exists near the morphotropic phase boundary (MPB) in the ceramics. The piezoelectric coefficient (d_{33}) measurement of the ceramics shows that the higher piezoelectric properties are corresponding to higher content of monoclinic phase.

Keywords: BZT-*x*BCT; X-ray techniques; Structural; Phase transitions

1. Introduction

$(1-x)BaZr_{0.2}Ti_{0.8}O_3-xBa_{0.7}Ca_{0.3}TiO_3$ (hereafter referred to as BZT-*x*BCT) ceramics exhibit high piezoelectric constant and are of potential interest as lead-free alternatives to $Pb(Zr,Ti)O_3$ (PZT). The piezoelectric coefficients (d_{33}) of BZT-*x*BCT ceramics with compositions near $x=0.5$ are around 560–620 pm/V, [1] higher than that of soft PZT, and these compositions have attracted much attention. The enhanced piezoelectric properties are closely related to composition-, stress-, temperature- and electric field-driven phase transitions. This means that the higher electromechanical responses have generally been obtained in the vicinity of the tetragonal and rhombohedral phase boundary (or the morphotropic phase boundary, MPB), and the phase transition near the MPB has been extensively investigated [2–6]. Liu and Ren [1,7] reported that the phase diagram of BZT-*x*BCT is similar to that of PZT, and the strong electromechanical responses are related to phase transitions close to the C–R–T tricritical point (where C, R and T represent cubic, rhombohedral and tetragonal phases, respectively). Since then, many studies have focused on the mechanism of the large piezoelectric effect in the BZT-*x*BCT system.

Damjanovic et al. [8] have reported that there is a special region near the MPB in the BZT-*x*BCT system, and dependence of the dielectric properties on temperature in the region cannot be fully explained by the T–R phase transition. While the phase composition in this region is controversial, it has been suggested that T- and R-phases coexist [9,10], T- and monoclinic (M)-phases coexist [11], or that orthogonal (O)-phase is present [12]. Ehmke et al. [13,14] have indicated that the phase composition under stress may be more complex than that previously reported for the BZT-*x*BCT system. The different phase compositions obtained in ceramics with the same atomic composition may be because of different manufacturing processes. Therefore, the different phase compositions and transitions caused by different manufacturing processes in the BZT-*x*BCT system should be studied. In the present study, the phase compositions and transitions in BZT-*x*BCT powders and ceramic pellets near the MPB were studied.

2. Experimental procedures

2.1. Sample preparation

Polycrystalline BZT-*x*BCT samples (with compositions x=0.46, 0.48, 0.50 and 0.52) were synthesized by a conventional solid state

*Corresponding author. Tel.: +86 541 8641 3908.
E-mail address: wdfei@hit.edu.cn (W.D. Fei).

0272-8842/$ - see front matter © 2013 Elsevier Ltd and Techna Group S.r.l. All rights reserved.
http://dx.doi.org/10.1016/j.ceramint.2013.08.037

reaction technique. Stoichioimetric quantities of $BaCO_3$ (99%), TiO_2 (98%), $CaCO_3$ (99%) and $BaZrO_3$ (99%) were mixed and ground by ball milling for 10 h with the addition of ethanol. After drying, the powder mixtures were calcined at 1250 °C for 3 h in air. Then, the mixture was ground again for 10 h. After drying, each powder mixture was divided into two parts; one part was mixed with PVA binder (wt%=3%) and pressed into pellets (10 mm diameter and 1 mm thick) under uniaxial stress, the other part remained unchanged. The pellet samples and powder samples were both sintered at 1400 °C for 3 h in air.

2.2. Experiment methods

XRD (to assess phase purity) was performed on a Philips X'pert X-ray diffractometer with Cu *K*α radiation at 40 kV and 40 mA. Before XRD tests, the pellet samples were polished and then annealed to eliminate the effect of polishing [15]. The refinement of diffraction peak profile was used to determine the phases. The observed (2 0 0) pc reflections of the samples were fitted to a pseudo-cubic coordinate system. During the peak-fitting procedure, a Pearson-VII function was used to define the profile shapes.

Silver electrodes were deposited on both sides of the pellet samples by magnetron sputtering. The dielectric properties were measured at 1 kHz as a function of temperature (−50–160 °C) using a Novocontrol CONCEPT40 Broadband Dielectric Spectrometer.

The samples were poled in a silicon oil bath at room temperature under an electric field of 3 kV/mm for the measurement of piezoelectric properties. Before measurement, the samples were placed at room temperature for 24 h, to remove any residual electric charge and make the samples more stable [16]. Piezoelectric constant d_{33} was measured by a quasi-static d_{33} meter (Model ZJ-4AN; Institute of Acoustics, Beijing, China).

The dielectric permittivity, ε', and loss tangent, tanδ, versus temperature are shown in Fig. 1a and b for ceramics with different compositions. The first derivatives of the real part of the dielectric permittivity versus temperature are shown in Fig. 1c. As shown in Fig. 1a–c, all samples have three dielectric anomaly peaks between −50 and 160 °C. Generally, peaks in dielectric property–temperature curves correspond to phase transitions [8], and therefore there are three phase transitions in our samples in this temperature range. The phase transition temperatures are presented in Fig. 1d, and the phase diagram (dashed line) given in a previous study [1] is also presented in the figure for comparison. It is clear that the phase transition at about 90 °C (solid squares in Fig. 1d) is the T-phase to C-phase transition, in agreement with the results of Liu et al. [1]. However, the phase transitions at lower temperatures (open circles and solid circles in Fig. 1d) are different from those in the previous study [1]. Obviously, the shadow region in Fig. 1d of our results cannot be interpreted as an R–T-phase transition.

3. Results and discussion

The XRD patterns of both powder and pellet samples are shown in Fig. 2(a) and (b), respectively. Both powder and

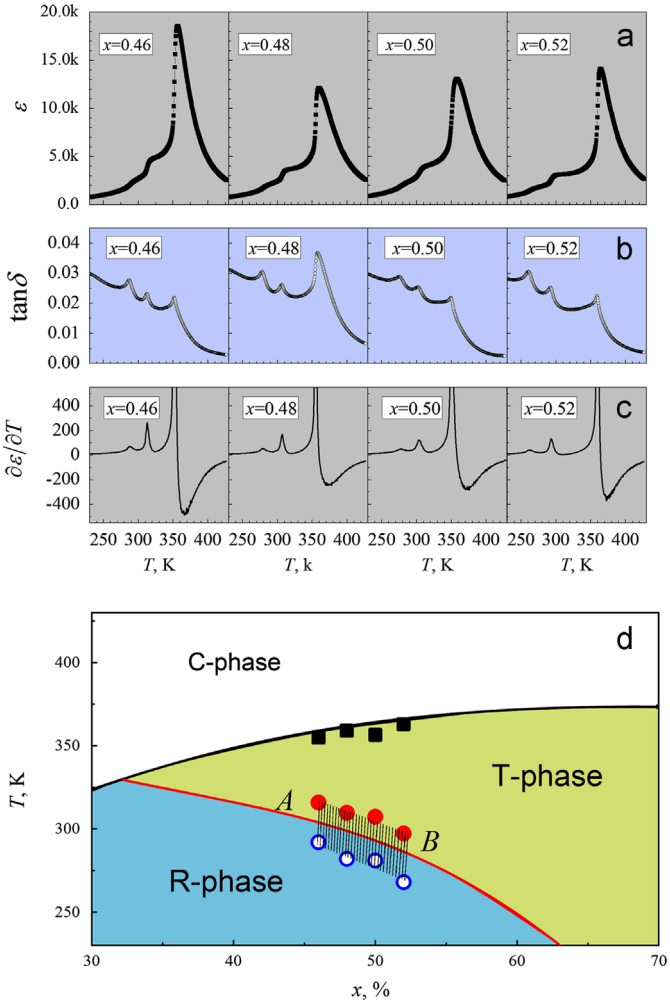

Fig. 1. Dielectric properties as a function of temperature (a) Dielectric permittivity ε' versus temperature for various compositions. (b) Corresponding losses, tanδ. (c) Derivative of the real part of the relative dielectric permittivity versus temperature. (d) Phase diagram based on ε' versus temperature data. Symbols are the peak temperatures from the curves in Fig. 1(c); smooth curves are data taken from Ref. [1].

pellet samples show pure perovskite structures. The full widths at half maxima of the peaks in the pellet samples are wider than those in the powder samples.

To further investigate the phase compositions, fine scan XRD were made. According to a review on the phase compositions in the lead free ferroelectric system [17], the possible p hases of this system are R-phase, T-phase, M-phase, O-phase, or their mixtures. The measured and fitted (to a pseudo-cubic coordinate system) profiles of the {2 0 0}pc reflections of powder and pellet samples are shown in Fig. 3. The measured profiles can be well simulated, and each of the (2 0 0)pc reflections of the powder samples required three peaks for a good fit.

Considering that there will be only one peak [(2 0 0)pc] for R-phase {2 0 0}pc reflection but two peaks [(0 0 2)pc and (2 0 0)pc] for T-, M- or O-phase {2 0 0}pc reflections, we propose that the three {2 0 0}pc reflection peaks in the powder samples indicate the coexistence of R-phase and another phase (referred to as A-phase). According to the lattice constants of

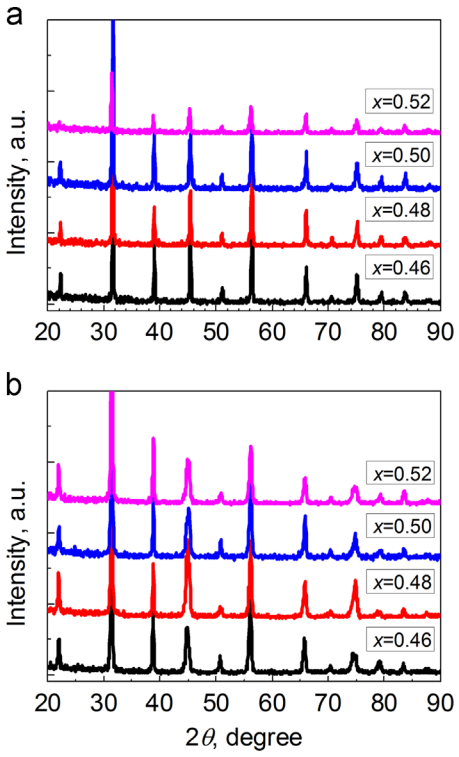

Fig. 2. Standard XRD patterns. (a) Reflections from powder samples. (b) Reflections from pellet samples.

the above phases, the middle peaks (olive lines in Fig. 3a–d) correspond to R-phase, and the other two peaks (blue lines in Fig. 3a–d) correspond to A-phase. As shown in Fig. 3a–d, the lower angle and higher angle peaks are defined as (0 0 2)pc and (2 0 0)pc peaks, and the intensity ratios of (0 0 2)pc and (2 0 0)pc ($I_{0\,0\,2}/I_{2\,0\,0}$) can be obtained. The values of $I_{0\,0\,2}/I_{2\,0\,0}$ are close to 1:2 for all powder samples. Therefore, A-phase may be T- or M-phase, but not O-phase, because $I_{0\,0\,2}/I_{2\,0\,0}$ is 2:1 for O-phase.

Moreover, the relative intensity of the {2 0 0}pc reflection of R-phase decreases and that of A-phase increases with increasing x, which suggests that R-phase is gradually transformed into A-phase. At the same time, the gap ($\Delta 2\theta$) between the (0 0 2)pc and (2 0 0)pc peaks for A-phase increases slightly, as shown in Fig. 4a, indicating that the lattice ratio c/a increases slightly with increasing x.

As shown in Fig. 3e–h, all {2 0 0}pc reflections of the pellet samples are split and broadened. The split and broadened peaks from the pellet samples can only be simulated using four peaks, and these peaks are different from those needed to fit the patterns from the powder samples. However, the gaps ($\Delta 2\theta$) between the two middle peaks (pink lines in Fig. 3e–h) of the four peaks are quite closed to those found for A-phase in the powder samples. Therefore, we regard these two middle peaks as corresponding to A-phase in both the powder and pellet samples. Apart from the two middle peaks, the two

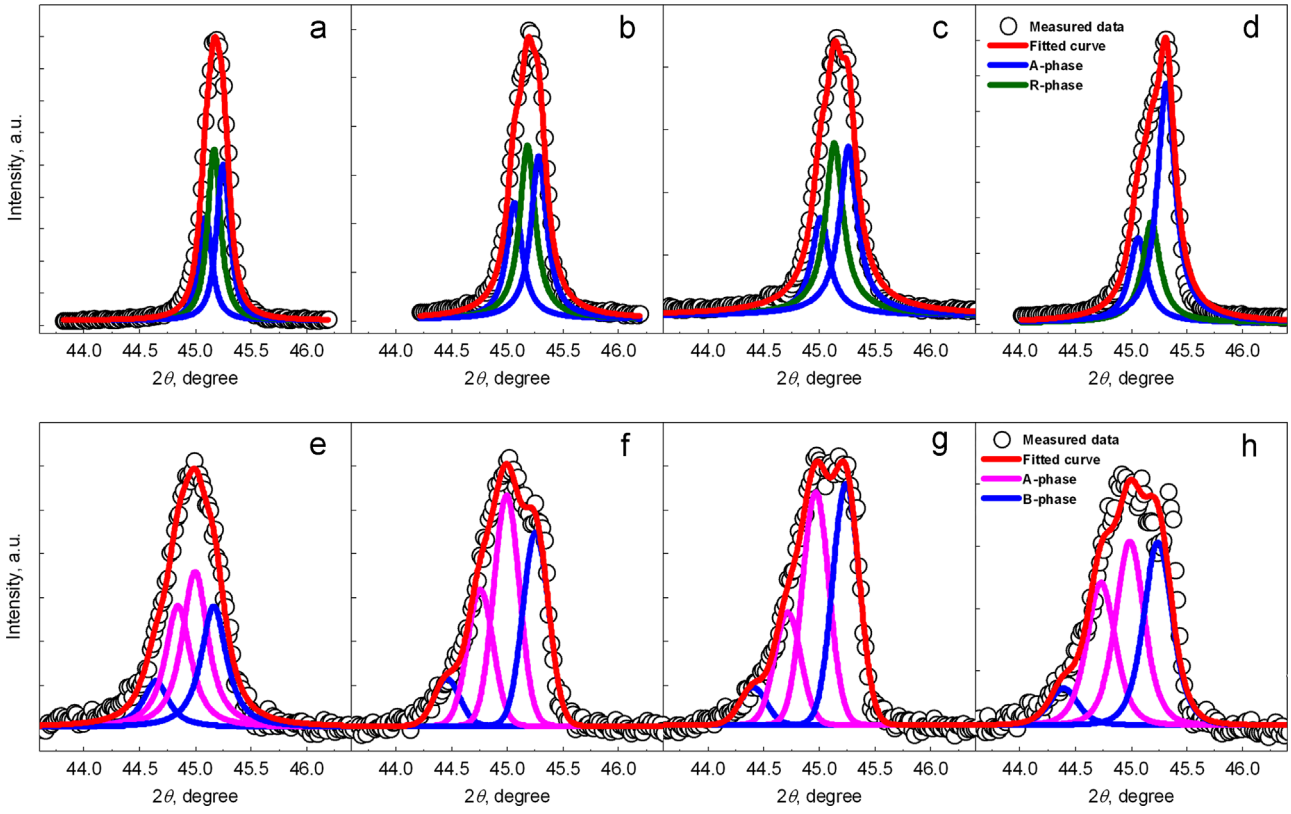

Fig. 3. Observed and calculated profiles of (2 0 0)pc reflections in a pseudo-cubic coordinate system. (a)–(d) Result of powder sample. (e)–(h) Result of pellet samples. (For interpretation of the references to color in this figure legend, the reader is referred to the web version of this article.)

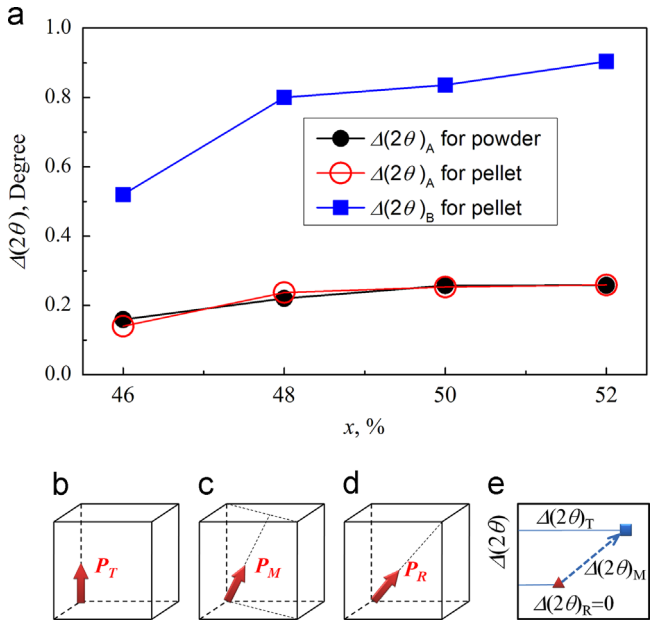

Fig. 4. (a) $\Delta 2\theta$ of A-phase and B-phase for powder and pellet samples; these values show that A-phase is in fact M-phase, while B-phase is T-phase. (b) Polar direction of T-phase. (c) Polar direction of M-phase. (d) Polar direction of R-phase. (e) $\Delta 2\theta$ of R-, M- and T-phases.

outermost peaks (blue lines in Fig. 3e–h) are defined as B-phase.

To further confirm the phase compositions, a comparison of the peak gaps ($\Delta 2\theta$) between the (0 0 2)pc and (2 0 0)pc peaks of A- and B-phases in pellet and powder samples is shown in Fig. 4a. The $\Delta(2\theta)_B$ values for the pellet are larger than the $\Delta(2\theta)_A$ values for both pellet and powder samples, while the $\Delta(2\theta)_A$ values for pellet and powder samples are almost the same. The polarization directions of T-, M- and R-phases are given in Fig. 4b–d. Based on polarization direction analysis, the order of peak spacings should be $\Delta(2\theta)_T > \Delta(2\theta)_M > \Delta(2\theta)_R = 0$ for {2 0 0}pc reflections, as is shown in Fig. 4e, when the chemical compositions are the same. Because the largest $\Delta(2\theta)$ value in the pellet sample is that of B-phase, B-phase can be assigned as T-phase. A-phase is most probably M-phase for both powder and pellet samples.

Therefore, the shadow region in the phase diagram of Fig. 1d for powder samples is a mixture of R- and M-phases, rather than R- and T-phases or a single phase [9,10,12]. The phase composition of pellet samples in the same region is a mixture of T- and M-phases, similar to that reported previously [11]. Therefore, the three peaks in the dielectric properties as a function of temperature for pellet samples can be interpreted as follows: the peak at lowest temperature corresponds to the R–M phase transition; the peak at intermediate temperature corresponds to the M–T phase transition and the peak at the highest temperature can be assigned to the T–C phase transition. In addition, the difference in phase composition between powder and pellet samples probably results from residual stress in the pellet sample [18]. This residual stress in the pellet samples can be confirmed by the shift of {2 0 0}pc peaks to lower angles for pellet samples compared with powder samples of the same composition.

Piezoelectric constants (d_{33}) of the pellet samples have been tested. BZT-0.46BCT has the lowest d_{33}, ~310pc/N, BZT-0.48BCT has the highest d_{33}, ~460pc/N at room temperature. For BZT-0.50BCT and BZT-0.52BCT, the d_{33} volume are 410 and 360 pc/N, respectively. The d_{33} values of BZT-0.48BCT and BZT-0.50BCT are obviously larger than those of the other pellets. As shown in Fig. 3e–h, the relative contents of M-phase (A-phase) in BZT-0.48BCT and BZT-0.50BCT pellets are higher than those in the other pellets, which means that the higher piezoelectric properties of these pellets may be related to the presence of M-phase. Crystallographically, M-phase is a subgroup of both R- and T-phases, which would provide a way for R-phase to transform into T-phase. In addition, the polarization direction of M-phase can be rotated in the (1 $\bar{1}$ 0)pc plane; this rotation is known to contribute to the high piezoelectric properties of the PZT system [19–22]. We propose that the origin of the huge piezoelectric response in BZT-xBCT is similar to that in PZT, that is, polarization rotation of M-phase.

Importantly, we found that the phase transitions of the BZT-xBCT ceramic system are very sensitive to stresses, in other words, the phase compositions may be totally different when there are small differences in the stress conditions of the samples. Our results suggest that the accurate measurements of phase compositions of BZT-xBCT ceramics near MPB are difficult, because the stress differences are very difficult to avoid.

4. Conclusions

In summary, dielectric and piezoelectric properties and phase transitions of BZT-xBCT ceramic systems have been investigated. The high piezoelectric responses are closely related to the existence of M-phase. The phase transitions of BZT-xBCT ceramic systems are very sensitive to stress, making accurate measurements of phase compositions of BZT-xBCT ceramics near the MPB difficult.

Acknowledgements

The research was financially supported by the National Natural Science Foundation of China (No: 11272102).

References

[1] W. Liu, X. Ren, Large piezoelectric effect in Pb-free ceramics, Physical Review Letters 103 (2009).
[2] M. Ahart, M. Somayazulu, R.E. Cohen, P. Ganesh, P. Dera, H.K. Mao, R.J. Hemley, Y. Ren, P. Liermann, Z. Wu, Origin of morphotropic phase boundaries in ferroelectrics, Nature 451 (2008) 545–548.
[3] F. Zheng, J. Chen, X. Li, M. Shen, Morphotropic phase boundary (MPB) effect in Pb (Zr,Ti)O_3 rhombohedral/tetragonal multilayered films, Materials Letters 60 (2006) 2733–2737.
[4] Q. Li, Y. Zhang, Z. Xia, X. Chu, MPB design and crystal growth of PMN–PT–PZ relaxor ferroelectrics, Journal of Crystal Growth 318 (2011) 851–855.

[5] J. Shieh, K.C. Wu, C.S. Chen, Switching characteristics of MPB compositions of $(Bi_{0.5}Na_{0.5})TiO_3$–$BaTiO_3$ –$(Bi_{0.5}K_{0.5})TiO_3$ lead-free ferroelectric ceramics, Acta Materialia 55 (2007) 3081–3087.

[6] E.B. Araújo, E.C. Lima, J.D.S. Guerra, A.O. dos Santos, L.P. Cardoso, M.U. Kleinke, Evidence for the monoclinic–tetragonal phase coexistence in $Pb(Zr_{0.53}Ti_{0.47})O_3$ thin films, Journal of Physics: Condensed Matter 20 (2008) 415203.

[7] H. Bao, C. Zhou, D. Xue, J. Gao, X. Ren, A modified lead-free piezoelectric BZT–xBCT system with higher T_C, Journal of Physics D: Applied Physics 43 (2010) 465401.

[8] D. Damjanovic, A. Biancoli, L. Batooli, A. Vahabzadeh, J. Trodahl, Elastic, dielectric, and piezoelectric anomalies and Raman spectroscopy of $0.5Ba(Ti_{0.8}Zr_{0.2})O_3$-$0.5(Ba_{0.7}Ca_{0.3})TiO_3$, Applied Physics Letters 100 (2012) 192907.

[9] J. Gao, D. Xue, Y. Wang, D. Wang, L. Zhang, H. Wu, S. Guo, H. Bao, C. Zhou, W. Liu, S. Hou, G. Xiao, X. Ren, Microstructure basis for strong piezoelectricity in Pb-free $Ba(Zr_{0.2}Ti_{0.8})O_3$–$(Ba_{0.7}Ca_{0.3})TiO_3$ ceramics, Applied Physics Letters 99 (2011) 092901.

[10] A. Bjørnetun Haugen, J.S. Forrester, D. Damjanovic, B. Li, K. J. Bowman, J.L. Jones, Structure and phase transitions in $0.5(Ba_{0.7}Ca_{0.3}$-$TiO_3)$–$0.5(BaZr_{0.2}Ti_{0.8}O_3)$ from −100 °C to 150 °C, Journal of Applied Physics 113 (2013) 014103.

[11] P. Mishra, Sonia, P. Kumar, Effect of sintering temperature on dielectric, piezoelectric and ferroelectric properties of BZT–BCT 50/50 ceramics, Journal of Alloys and Compounds 545 (2012) 210–215.

[12] D.S. Keeble, F. Benabdallah, P.A. Thomas, M. Maglione, J. Kreisel, Revised structural phase diagram of $(Ba_{0.7}Ca_{0.3}TiO_3)$–$(BaZr_{0.2}Ti_{0.8}O_3)$, Applied Physics Letters 102 (2013) 092903.

[13] M.C. Ehmke, S.N. Ehrlich, J.E. Blendell, K.J. Bowman, Phase coexistence and ferroelastic texture in high strain $(1-x)Ba(Zr_{0.2}Ti_{0.8})O_3$–$x(Ba_{0.7}Ca_{0.3})TiO_3$ piezoceramics, Journal of Applied Physics 111 (2012) 124110.

[14] M.C. Ehmke, J. Daniels, J. Glaum, M. Hoffman, J.E. Blendell, K. J. Bowman, Reduction of the piezoelectric performance in lead-free $(1-x)Ba(Zr_{0.2}Ti_{0.8})O_3-x(Ba_{0.7}Ca_{0.3})TiO_3$ piezoceramics under uniaxial compressive stress, Journal of Applied Physics 112 (2012) 114108.

[15] W. Chang, A.H. King, K.J. Bowman, Effects of residual (or internal) stress on ferroelectric domain wall motion in tetragonal lead titanate, Journal of Materials Research 22 (2011) 2845–2850.

[16] S. Su, R. Zuo, S. Lu, Z. Xu, X. Wang, L. Li, Poling dependence and stability of piezoelectric properties of $Ba(Zr_{0.2}Ti_{0.8})O_3$–$(Ba_{0.7}Ca_{0.3})TiO_3$ ceramics with huge piezoelectric coefficients, Current Applied Physics 11 (2011) S120–S123.

[17] J. Rödel, W. Jo, K.T.P. Seifert, E.-M. Anton, T. Granzow, D. Damjanovic, Perspective on the development of lead-free piezoceramics, Journal of the American Ceramic Society 92 (2009) 1153–1177.

[18] G. Xu, J. Wen, C. Stock, P.M. Gehring, Phase instability induced by polar nanoregions in a relaxor ferroelectric system, Nature Materials 7 (2008) 562–566.

[19] R. Ragini, S.K. Ranjan, Mishra, D. Pandey, Room temperature structure of $Pb(Zr_xTi_{1-x}O_3)$ around the morphotropic phase boundary region: a Rietveld study, Journal of Applied Physics 92 (2002) 3266.

[20] M. Fornari, D. Singh, Possible coexistence of rotational and ferroelectric lattice distortions in rhombohedral $PbZr_xTi_{1-x}O_3$, Physical Review B: Condensed Matter 63 (2001).

[21] J. Frantti, S. Ivanov, S. Eriksson, H. Rundlöf, V. Lantto, J. Lappalainen, M. Kakihana, Phase transitions of $Pb(Zr_xTi_{1-x})O_3$ ceramics, Physical Review B: Condensed Matter 66 (2002).

[22] A. Souza Filho, K. Lima, A. Ayala, I. Guedes, P. Freire, F. Melo, J. Mendes Filho, E. Araújo, J. Eiras, Raman scattering study of the $PbZr_{1-x}Ti_xO_3$ system: rhombohedral–monoclinic–tetragonal phase transitions, Physical Review B: Condensed Matter 66 (2002).